Article

SOLID-STATE SPECTROSCOPIC, THERMOKINETICS AND THERMAL ANALYSIS OF ACECLOFENAC COORDINATION COMPLEXES WITH LANTHANUM AND GADOLINIUM

Laís D. S. M. K. Melo[a], Cláudio T. Carvalho[a], Pedro Enrique Sánchez Jiménez[b,c], Thiago Sequinel[a], Antonio Perejón[b,c], Luis Allan Pérez Maqueda[b] and Tiago A. D. Colman[a,*]

[a]Faculdade de Ciências Exatas e Tecnologia, Universidade Federal da Grande Dourados (UFGD), 79804-970 Dourados – MS, Brasil

[b]Department of Inorganic Chemistry, University of Seville, 41092 Sevilla, Spain

[c]Materials Science Institute, Spanish National Research Council (CSIC), University of Seville, CP 41092 Seville, Spain

Received: 09/22/2023; accepted: 01/15/2024; published online: 05/24/2024

In recent years, the field of coordination chemistry has experienced a surge in interest regarding the synthesis and characterization of coordination complexes for diverse applications. This study is dedicated to investigating coordination compounds resulting from the interaction of nonsteroidal anti-inflammatory drugs (NSAIDs) with metal ions. The study research places significant emphasis on understanding the stability and thermal behavior of these coordination compounds. The utilization of thermoanalytical techniques is crucial in achieving this goal. Thermal analysis and thermokinetics provide valuable insights into the underlying mechanisms, kinetics, and energetics of these reactions, thereby facilitating the optimization of synthesis procedures. The research employs concurrent techniques, namely thermogravimetric analysis (TG) and differential scanning calorimetry (DSC), to explore the thermal stability and decomposition pathways of these coordination compounds. Thermokinetic models and optimization methodologies are subsequently applied to identify key reaction parameters. The primary aim of this research is to unveil the thermal behavior, stability, and reaction kinetics of aceclofenac coordination compounds, thus contributing significantly to the understanding of thermokinetics and thermal analysis in the domain of coordination chemistry. Specifically, this study is focused on aceclofenac coordination complexes involving lanthanum and gadolinium, with the ultimate goal of advancing the field of coordination chemistry.

Keywords: thermal analysis; thermogravimetry; metallopharmaceuticals.

INTRODUCTION

The field of coordination chemistry has received substantial progress in recent years, with a growing interest in the synthesis and characterization of coordination complexes for diverse applications. One area of interest within this field is the study of coordination complexes formed between nonsteroidal anti-inflammatory drugs (NSAIDs) with metal ions. These complexes have shown potential as modulators of inflammatory and autoimmune responses.[1-5]

Aceclofenac, a widely used NSAID, has been the subject of extensive research due to its therapeutic properties and potential side effects. Previous studies[1,6-9] have demonstrated that the complexation of aceclofenac with zinc results in a zinc-aceclofenac complex that exhibited reduced stomach ulceration in animal models while maintaining comparable anti-inflammatory activity. This finding suggests that coordination complexes formed by aceclofenac with other metal ions may also possess unique properties and could be explored for their potential therapeutic applications.

The application of thermokinetics and thermal analysis to solid-state reactions plays a crucial role in understanding the thermal behavior and stability of coordination complexes. These studies offer valuable insights into the reaction mechanisms, kinetics, and energetics involved in the formation and decomposition of these complexes.[10-12]

To achieve this goal, a combination of experimental techniques and computational methods were employed. Thermogravimetric analysis (TG) and differential scanning calorimetry (DSC) were used to investigate the thermal stability and decomposition pathways of the coordination complexes. The data obtained were analyzed using state-of-the-art thermokinetic models and nonparametric variational optimization methods.[13] These approaches allow for the determination of reaction coordinates and the optimization of reaction mechanisms without the need for a priori assumptions about the functional form of the reaction coordinate.[13] In a related study, Souza *et al.*[14] conducted a comprehensive investigation involving the synthesis, characterization, and thermoanalytical study of aceclofenac coordination complexes with light lanthanides (La, Ce, Pr, and Nd) in the solid state. The authors investigated the thermal behavior and stability of these complexes using simultaneous thermogravimetric analysis (TG) and differential scanning calorimetry (DSC). The findings from their research provided valuable insights into the thermal properties and decomposition pathways of these complexes, contributing significantly to the understanding of their potential applications in the field of coordination chemistry.

This study aims to elucidate the thermal behavior, stability, and reaction kinetics of these coordination compounds, utilizing a combination of experimental techniques and computational calculations. The findings of this investigation have the potential to contribute to the development of novel coordination compounds, thereby paving the way for further investigations in the field of coordination chemistry.

EXPERIMENTAL

Materials and synthesis of compounds

The materials used for the synthesis of the compounds included lanthanum oxide (CAS number1312-81-8, Sigma-Aldrich, purity > 99.5%), gadolinium oxide (CAS number 12064-62-9, Sigma-Aldrich, purity > 99.5%), acelofenac (CAS number 89796-99-6, Sigma-Aldrich, purity > 98%), hydrochloric acid (CAS number 7647-01-0, Merck, 37%), and ammonium hydroxide

*e-mail: tiagocolman@ufgd.edu.br

(CAS number 1336-21-6, BioUltra, 28%). The synthesis of the compounds followed the methodology described in the literature by Souza *et al.*[14]

Spectroscopic characterization mid-infrared with Fourier transform (FTIR)

The FTIR spectra were recorded at 16 scans *per* spectrum with a resolution of 4 cm^{-1} using a Nicolet iS 10 FTIR spectrophotometer (Thermo Fisher Scientific, Waltham, USA) equipped with an attenuated total reflectance (ATR) accessory featuring a Ge window. Subsequently, FTIR spectra were re-recorded at a heightened precision of 32 scans *per* spectrum, maintaining a resolution of 4 cm^{-1}.[14,15]

Simultaneous thermogravimetric analysis-differential scanning calorimetry (TG-DSC)

The TG curves were registered using a thermogravimetric equipment, Netzsch STA449 F1 Jupiter® (Netzsch, Selb, Germany), which was properly calibrated following the manufacturer's instructions and controlled by the Proteus® software. The analysis of the samples was conducted under the conditions presented in Table 1, utilizing a α-alumina crucible with a volume of 70 µL.[14,16-18] The experiments were carried out with a compressed air flow of 50 mL min^{-1} and heating in the range of 30-1000 °C, employing heating rates of 2, 4, 6, 8, and 10 °C min^{-1}.

Table 1. Masses used in the different heating rates for each compound in the kinetic studies

Heating ratio / (°C min^{-1})	Mass of sample / mg	
	La compound	Gd compound
2	2.9963	2.9678
4	2.9816	2.9874
6	2.9658	2.9318
8	2.9785	2.9538
10	2.9815	2.9843

La: lanthanum; Gd: gadolinium.

RESULTS AND DISCUSSION

Spectroscopic characterization

The FTIR spectra of all compounds share a striking similarity, portrayed in Figure 1. The analyses were crafted by exploring potential coordination sites and consulting pertinent literature.[14,15,18] Guided by methodology of Deacon and Philips,[19] our focus is on bands considered fundamental for unravel metal-ligand coordination, especially within the carboxylate group: symmetric ($\nu_{sym}COO^-$) and asymmetric ($\nu_{asym}COO^-$) bands resonating between 1600 and 1300 cm^{-1}.

To comprehend the interaction between the lanthanides and the ligand, we examined the assignment of symmetric and asymmetric bands of the carboxylate group, drawing parallels to the sodium salt of aceclofenac. Interplay unfolds with a medium-intensity at 1600 cm^{-1} and a robust resonance at 1450 cm^{-1}, embodying the asymmetric and symmetric bands of the carboxylate group. A comparative analysis of Δ ($\nu_{asym}COO^- - \nu_{sym}COO^-$) between the sodium salt and our synthesized compounds reveals a greater difference, hinting at a coordination where the carboxylate group engages in bridging and/or chelating interactions with the metal center.[14,19] More relevant bands are shown in Table 2.[14]

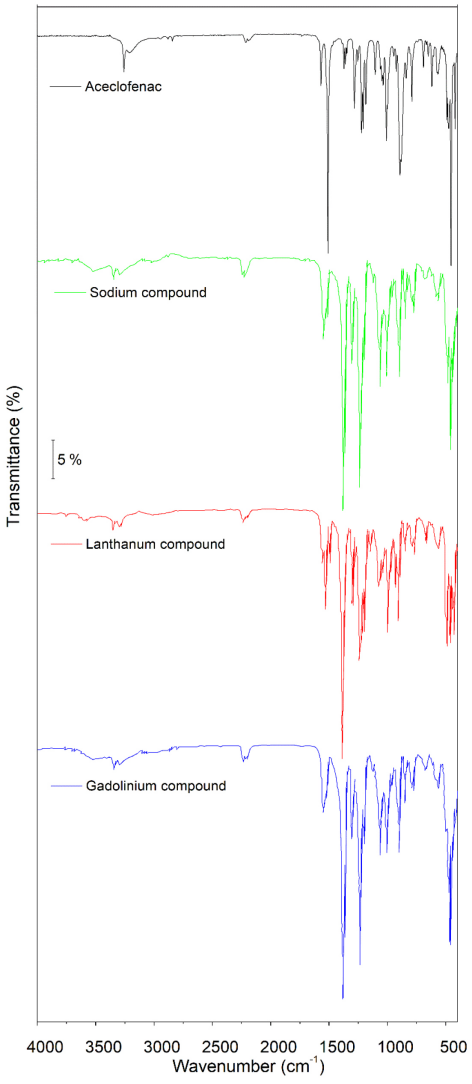

Figure 1. *FTIR spectra*

Thermoanalytical characterization of the lanthanum and gadolinium compounds

The simultaneous TG-DSC curves of the trivalent lanthanum compound under an air atmosphere, obtained at a heating rate of 2 °C min^{-1} are shown in Figure 2.

Table 2. FTIR assignments of the synthesized compounds

Compound	Functional group					
	$\nu N–H_{aromatic}$	$\nu_{asym}COO^-$	$\nu_{sym}COO^-$	νC–C	νC–Cl	Δν ($\nu_{asym}COO^- - \nu_{sym}COO^-$)
$Na(L)_3$		1600	1450	1070	780	
$[La(L)_3.4H_2O]$	3380	1590	1450	1080	770	140
$[Gd(L)_3.2.5H_2O]$	3370	1580	1450	1100	760	130

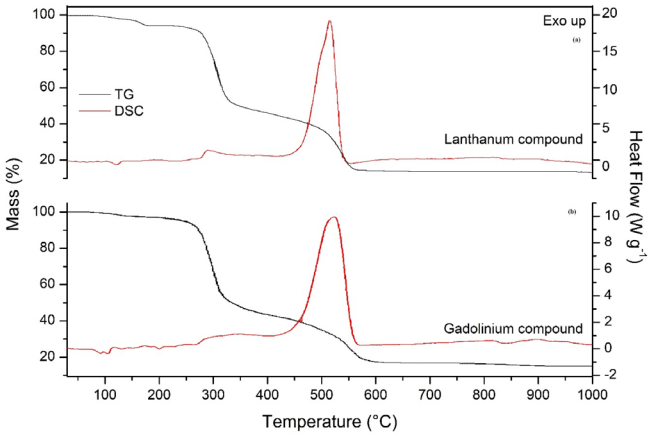

Figure 2. *(a) TG-DSC curves of lanthanum compound (m = 2.9963 mg) and (b) gadolinium compound (m = 2.9678 mg)*

The mass loss occurs in four steps on the TG curve, and endothermic and exothermic events are observed in the DSC curve. The results of these curves are presented in Table 3.

Table 3. TG-DSC results for the lanthanum compound

Parameter	TG-DSC stages			
	1st	2nd	3rd	4th
θ / °C	30-150	225-350	350-560	545-700
Tp / °C	128 ↓	278 ↑	513 ↑	
Δm / %	5.89	45.06	34.41	1.23

Temperature range (θ); peak temperature (Tp) and mass loss (Δm) observed in the TG-DSC curves. Exothermic event (↑); endothermic event (↓).

The first mass loss occurred between 30-140 °C, corresponding to the endothermic peak at 128 °C attributed to dehydration of the compound, resulting in a loss of 5.89% in mass associated with the removal of 4 H_2O molecules. This step is followed by the thermal stability of the anhydrous compound, $La(L)_3$, up to 188 °C. Above this temperature, the TG curve suggests 3 steps of consecutive binder to lanthanum oxide formation. The second mass loss took place in the range of 225-350 °C with a mass loss of 45.06%, corresponding to a small exothermic peak at 300 °C.

The third stage occurred between 350 and 560 °C with a mass loss of 34.41%, corresponding to a large exothermic peak at 513 °C, indicative of the oxidation of organic matter and/or the release of gaseous products during thermal decomposition. This process leads to the formation of carbonaceous and/or carbonate-derived residues. The first, second, and third stages of thermal decomposition of the lanthanum compound are consistent with the findings reported by Souza *et al.*[14] The fourth stage occurred between 545 and 700 °C, showing an observed mass loss of 1.23%, which can be attributed to the final oxidation temperature where organic matter and/or gaseous products that evolve during the thermal decomposition of the anhydrous compound. This process also coincides with the complete formation of the corresponding lanthanide oxide, as confirmed by X-ray diffractometry using the powder method.

The La_2O_3 formed accounts for 13.41% of the mass of the compound. It should be noted that the stoichiometry of compounds will be discussed in more depth in "Stoichiometry of compounds" sub-section. The DSC curve does not show any evidence of endothermic (decomposition of carbonate derivatives) or exothermic events (oxidation of carbonized waste) associated with this mass loss. Probably the events occurred simultaneously, and the heat produced was not sufficient to be observed in the DSC curve, as has already been observed in other lanthanide compounds.[14,18]

Thermoanalytical characterization of gadolinium compound

The simultaneous TG-DSC curves of the trivalent gadolinium compound under an air atmosphere, obtained at a heating rate of 2 °C min^{-1}, are shown in Figure 2.

Mass loss occurs in four steps in the TG curve, and the endothermic and exothermic events are observed by the DSC curve. The results of the curves are presented in Table 4. A certain degree of similarity is observed between the curves of the La and Gd complexes, as observed in other trivalent lanthanide compounds.[20]

Table 4. TG-DSC results for the gadolinium compound

Parameter	TG-DSC stages			
	1st	2nd	3rd	4th
θ / °C	70-150	190-340	340-620	620-915
Tp / °C	95 ↓, 108 ↓	213 ↓, 270 ↓	525 ↑	
Δm / %	3.30	46.12	33.63	1.77

Temperature range (θ); peak temperature (Tp) and mass loss (Δm) observed in the TG-DSC curves. Exothermic event (↑); endothermic event (↓).

The first mass loss occurred between 70-150 °C with a loss of 3.30% associated with the removal of 2.5 water molecules. This is indicated by the endothermic peaks at temperatures of 95 and 108 °C, attributed to the dehydration of the compound, followed by the thermal stability of the anhydrous compound $Gd(L)_3$ up to 190 °C. Subsequently, the thermal decomposition of this compound is observed in 3 consecutive steps, as was observed for another anhydrous compound of Gd(III).[20]

The second stage of the thermal decomposition of the anhydrous compound occurred in the range of 190-340 °C with a mass loss of 46.12%. This corresponds to a small endothermic peak at 213 and 270 ºC, related to the thermal decomposition.The third stage occurred between 340-620 °C with a mass loss of 33.63%, corresponding to the broad and significant exothermic peak attributed to the oxidation of organic matter and/or gaseous products that evolve during thermal decomposition with the formation of carbonaceous and/or carbonate-derived residues. Finally, the fourth step occurred between 620-915 °C, attributed as the final temperature of the oxidation of organic matter and/or gaseous products evolved during thermal decomposition, resulting in the complete formation of the respective gadolinium oxide (Gd_2O_3). This step involves a mass loss of 1.77%, with a thermal event occurring between 800-850 °C associated with the decomposition of the carbonaceous residue.

The TG-DSC curves of the studied complexes showed that the thermal stability and the final temperature of thermal decomposition depend on the nature of the metal ions. It was observed that, for the studied compounds, the gadolinium compound exhibited greated stability than the lanthanum compound.

Stoichiometry of compounds

The data presented in Tables 3 and 4 were used to calculate the stoichiometry of the complexes, considering the percentages associated with hydration waters, the loss of mass of the ligand, and the percentage of residue (oxide). The stoichiometry was determined by calculating the minimum formula. As an example, the calculation for the lanthanum complex ($La_x(L_y)\cdot nH_2O$) is provided below as a representative illustration:[17]

(*i*) Divide the loss of mass or residue (TG) by the corresponding molar mass (1st calculation step);

(*ii*) The smallest value found in the first step will be the common divisor (2nd calculation step).

1st calculation step

H_2O: 5.89/18.02 (H_2O) = 0.327
Δligand: 80.70/353.18 (Acec – 1 hydrogen) = 0.228
Residue: 13.41/162.90 (1/2 La_2O_3) = 0.082

2nd calculation step

H_2O: 0.0,327/0.082 = 3.9 ≈ 4
Δligand: 0.229/0.082 = 2.8 ≈ 3
Residue (1/2 La_2O_3) = 0.082/0.082 = 1.0

The following stoichiometry was found to the lanthanum complex: $[La(L)_3.4H_2O]$, and gadolinium complex: $[Gd(L)_3.2.5H_2O]$, where L represents the aceclofenac ligand. The total mass loss was calculated theoretically for both complexes and the values obtained are summarized in Table 5 together with the values calculated from the thermogravimetric data. From these data, it was also possible to estimate the purity level of these complexes (Table 5).

Table 5. Results of total mass loss and purity of the compounds

Compound	Mass loss (Δm) / %		Purity / %
	Calculated	TG	
$La(L)_3.4H_2O$	84.22	86.59	97.26
$Gd(L)_3.2.5H_2O$	86.44	84.82	98.13

The total mass losses correlated with the formation of the respective oxides, with 13.41% for La_2O_3 and 15.18% for Gd_2O_3. By analyzing the percentages of mass loss, the amount in milligrams of the lost mass was determined. This information was then used to assess the purity of the complexes. The determined purities were satisfactory, as they meet the minimum purity requirement of 95% established by the Brazilian Pharmacopoeia.[21]

Kinetic study

Through the bibliographic review, the optimal experimental conditions for conducting the kinetic analysis were determined based on the most used parameters in kinetic characterization, along with recommendations of the International Confederation for Thermal Analysis and Calorimetry (ICTAC) experiments.[22-25] The amount of sample used was approximately 3.00 mg for both compounds, a common practice in the literature[22,26,27] that ensures the TG equipment can achieve accurate analysis measurements, with as homogeneous heating as possible in the sample. The thermogravimetric analysis was conducted under non-isothermal conditions to obtain a temperature range capable of detecting the reaction profile in a single run, enabling faster analysis. The non-isothermal condition generated temperature-dependent results, and heating rates of 2, 4, 6, 8, and 10 °C min^{-1} were employed. The thermokinetic treatment was performed using the Thinks,[28] a free open-source thermokinetic software. The chosen methods were isoconversional analysis[29-32] and model fitting (linear regression).[33,34]

One of the ICTAC recommendations that is commonly used in the literature,[22,35] as the articles selected in the bibliographic survey point out, is that the kinetic analysis method chosen to determine the kinetic parameters shall include the step where the greatest mass loss occurs. Additionally, it allows determining the step to be studied or the analytical signal used. As the thermal decomposition of the studied compounds occurs in consecutive and/or overlapping steps, it was decided to calculate the kinetic parameters considering the entire thermal decomposition of the compounds.

Isoconversional analysis

The kinetic parameters for the studied coordination compounds were calculated by the Kissinger method (Equation 1).[29,30]

$$\ln\left(\frac{\beta_i}{T_{p,i}}\right) = \ln\frac{AR}{E_a} - \frac{E_a}{RT_{p,i}} \quad (1)$$

where β: heating rate; T: temperature; A: pre-exponential constant; R: gas constant, equal to 8.3144 J mol^{-1} K^{-1}; E_a: activation energy.

The apparent activation energies were determined by analyzing the dependence on the degree of conversion for each heating rate (β) *versus* the inverse of the temperature at each specific degree of conversion. All calculations and adjustments of the respective values of α for each β incorporated all steps of mass loss. The Kissinger plot, isoconversional plot of activation energy, and isoconvertional results are shown in Figure 3 for the lanthanum compound and in Figure 4 for the gadolinium compound.

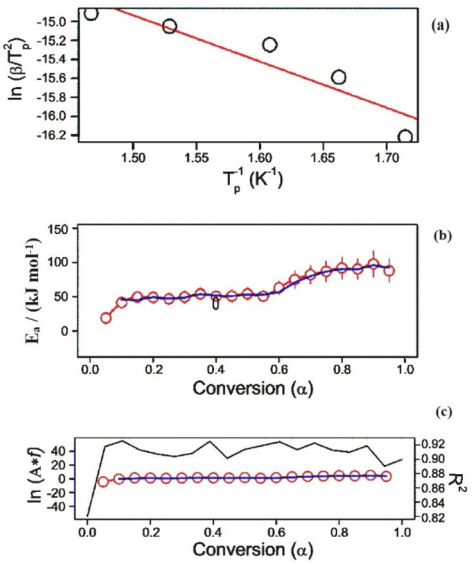

Figure 3. *Kissinger plot (a), isoconversional plot of activation energy (b), and isoconvertional results (c) for the lanthanum compound*

It is observed that the higher the heating rate, the greater the displacement of the curves and the lower the resolution of the steps. Therefore, one should work with heating rates as small as possible, thus avoiding highly displaced curves that lead to higher decomposition temperatures. Furthermore, the values of activation energy are significantly influenced by the fact that the decomposition of the compounds takes place in several overlapping stages. Table 6 presents the values of the activation energies calculated by the Kissinger method for each degree of conversion.

The activation energy values for the thermal decomposition of the compounds, obtained through the Kissinger method, were 40.51 ± 21.28 kJ mol^{-1} for the lanthanum compound and 35.45 ± 15.84 kJ mol^{-1} for the gadolinium compound.

Model fitting (linear regression)

The kinetic parameters estimated for the synthesized compounds

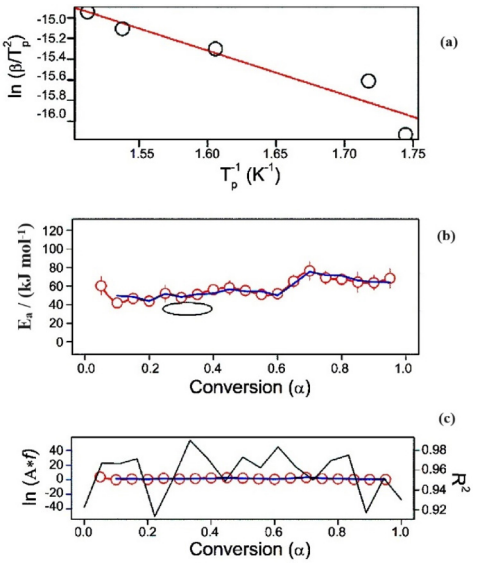

Figure 4. *Kissinger plot (a), isoconversional plot of activation energy (b), and isoconvertional results (c) for the gadolinium compound*

Table 6. Thermokinetics results obtained by the Kissinger method

Conversion (α)	Compound	
	$La(L)_3.4H_2O$ E_a / (kJ mol^{-1})	$Gd(L)_3.2.5H_2O$ E_a / (kJ mol^{-1})
0.05	19.06	60.24
0.10	41.55	41.74
0.15	49.41	46.79
0.20	49.06	43.82
0.25	46.87	52.06
0.30	49.50	47.63
0.35	54.11	50.96
0.40	50.60	56.22
0.45	50.96	58.14
0.50	54.32	55.22
0.55	50.76	50.97
0.60	62.98	51.83
0.65	75.20	65.25
0.70	82.21	76.38
0.75	87.07	68.95
0.80	92.01	67.22
0.85	90.48	64.20
0.90	97.88	63.66
0.95	87.94	68.32

E_a: activation energy.

by the model fitting method (linear regression) were calculated based on Equation 2.[33]

$$\ln\left(\frac{d\alpha}{dt}\right) - \ln\left[(1-\alpha)^n \alpha^m\right] = \ln(cA) - \frac{E_a}{RT} \quad (2)$$

where α: reaction fraction; A: pre-exponential constant; Ea: activation energy; R: gas constant, equal to 8.3144 J mol^{-1} K^{-1}; T: temperature.

The correlation between f(α)/f(0.5) and the conversion estimated by the fitting model (linear regression) is shown in Figure 5.

The model adopted for the analysis of the obtained data is based on the mechanisms of the type unimolecular decay law (instantaneous nucleation and unidimensional growth), where f(α) corresponds to 1 – α. Using the method adopted to calculate the kinetic parameters, an activation energy of 29.9 ± 2.7 kJ mol^{-1} was found for the lanthanum compound, and 37.2 ± 1.3 kJ mol^{-1} for the gadolinium compound.

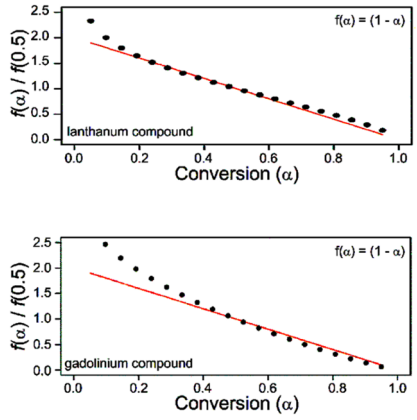

Figure 5. *Correlation between f(α)/f(0.5) and the conversion estimated by the model fitting method*

CONCLUSIONS

The thermal behavior results of lanthanum and gadolinium complexes exhibited a certain similarity, with stoichiometry determined by TG-DSC results corresponding to $La(L)_3.4H_2O$ and $Gd(L)_3.2.5H_2O$. Both complexes displayed four mass losses, including three stages of decomposition for the anhydrous compound. The gadolinium compound proved to be more stable and exhibited higher purity when compared to the lanthanum compound.

The experimental data demonstrated a good quality, making them suitable for application in kinetic analysis and the determination of the apparent activation energy for each coordination compound.

ACKNOWLEDGMENTS

This work is financially supported by Conselho Nacional de Desenvolvimento Científico e Tecnológico (CNPq process No. 402435/2022-2 and No. 200114/2022-0); Finaciadora de Estudos e Projetos (FINEP contract 04.13.0448.00/2013); Coordenação de Aperfeiçoamento de Pessoal de Nível Superior (CAPES); Universidade Federal da Grande Dourados (Edital PROPP-UFGD No. 01/02/2024).

REFERENCES

1. Leung, C. H.; Lin, S. H.; Zhong, H. J.; Ma, D. L.; *Chem. Sci.* **2015**, *6*, 871. [Crossref]
2. El-Tabl, A. S.; El-Waheed, M. M. A.; Wahba, M. A.; El-Fadl, N. A. H. A.; *Bioinorg. Chem. Appl.* **2015**, *2015*, 1. [Crossref]
3. Banerjee, A.; Mohanty, M.; Lima, S.; Samanta, R.; Garribba, E.; Sasamori, T.; Dinda, R.; *New J. Chem.* **2020**, *44*, 10946. [Crossref]
4. Parada, J.; Atria, A. M.; Baggio, R.; Wiese, G.; Lagos, S.; Pavón, A.; Rivas, E.; Navarro, L.; Corsini, G.; *J. Chil. Chem. Soc.* **2017**, *62*, 3746. [Crossref]
5. Ambika, S.; Manojkumar, Y.; Arunachalam, S.; Gowdhami, B.; Sundaram, K. K. M.; Solomon, R. V.; Venuvanalingam, P.; Akbarsha, M. A.; Sundararaman, M.; *Sci. Rep.* **2019**, *9*, 2721. [Crossref]
6. Guerra, R. B.; Fraga-Silva, T. F. C.; Aguiar, J.; Oshiro, P. B.; Holanda, B. B. C.; Venturini, J.; Bannach, G.; *Inorg. Chim. Acta* **2020**, *503*, 119408. [Crossref]

7. Ekawa, B.; Nunes, W. D. G.; Teixeira, J. A.; Cebim, M. A.; Ionashiro, E. Y.; Junior Caires, F.; *J. Anal. Appl. Pyrolysis* **2018**, *135*, 299. [Crossref]
8. Bao, G.; *J. Lumin.* **2020**, *228*, 117622. [Crossref]
9. Herlan, C.; Bräse, S.; *Dalton Trans.* **2020**, *49*, 2397. [Crossref]
10. Chaudhary, R. G.; Ali, P.; Gandhare, N. V.; Tanna, J. A.; Juneja, H. D.; *Arabian J. Chem.* **2019**, *12*, 1070. [Crossref]
11. MacCallum, J. R.; Tanner, J.; *Eur. Polym. J.* **1970**, *6*, 1033. [Crossref]
12. Logvinenko, V. A.; *J. Therm. Anal.* **1990**, *36*, 1973. [Crossref]
13. Banushkina, P.; Krivov, S. V.; *J. Chem. Phys*. **2015**, *143*, 18410. [Crossref]
14. de Souza, A. S.; Ekawa, B.; de Carvalho, C. T.; Teixeira, J. A.; Ionashiro, M.; Colman, T. A. D.; *Thermochim. Acta* **2020**, *683*, 178443. [Crossref]
15. Pires, M. A. A.; de Carvalho, C. T.; Colman, T. A. D.; *J. Serb. Chem. Soc.* **2024**, *89*, 335. [Crossref]
16. Teixeira, J. A.; Nunes, W. D. G.; Colman, T. A. D.; do Nascimento, A. L. C. S.; Caires, F. J.; Campos, F. X.; Gálico, D. A.; Ionashiro, M.; *Thermochim. Acta* **2016**, *624*, 59. [Crossref]
17. Campos, F. X.; Nascimento, A. L. C. S.; Colman, T. A. D.; Gálico, D. A.; Treu-Filho, O.; Caires, F. J.; Siqueira, A. B.; Ionashiro, M.; *J. Therm. Anal. Calorim.* **2016**, *123*, 91. [Crossref]
18. Teixeira, J. A.; Nunes, W. D. G.; do Nascimento, A. L. C. S.; Colman, T. A. D.; Caires, F. J.; Gálico, D. A.; Ionashiro, M.; *J. Anal. Appl. Pyrolysis* **2016**, *121*, 267. [Crossref]
19. Deacon, G.; Phillips, R. J.; *Coord. Chem. Rev.* **1980**, *33*, 227. [Crossref]
20. Campos, F. X.; Nascimento, A. L. C. S.; Colman, T. A. D.; Gálico, D. A.; Carvalho, A. C. S.; Caires, F. J.; Siqueira, A. B.; Ionashiro, M.; *Thermochim. Acta* **2017**, *651*, 73. [Crossref]
21. *Farmacopeia Brasileira*, 6ª ed.; Agência Nacional de Vigilância Sanitária (ANVISA): Brasília, 2019. [Link] accessed in April 2024
22. Vyazovkin, S.; Burnham, A. K.; Criado, J. M.; Pérez-Maqueda, L. A.; Popescu, C.; Sbirrazzuoli, N.; *Thermochim. Acta* **2011**, *520*, 1. [Crossref]
23. Drisya, R.; Soumyamol, U. S.; Chandran, P. R. S.; Sudarsanakumar, M. R.; Kurup, M. R. P.; *J. Therm. Anal. Calorim.* **2018**, *134*, 1987. [Crossref]
24. Logvinenko, V. A.; Sapchenko, S. A.; Fedin, V. P.; *J. Therm. Anal. Calorim.* **2016**, *123*, 697. [Crossref]
25. Logvinenko, V.; Zavakhina, M.; Bolotov, V.; Pishchur, D.; Dybtsev, D.; *J. Therm. Anal. Calorim.* **2017**, *130*, 335. [Crossref]
26. Koga, N.; Vyazovkin, S.; Burnham, A. K.; Favergeon, L.; Muravyev, N. V.; Pérez-Maqueda, L. A.; Saggese, C.; Sánchez-Jiménez, P. E.; *Thermochim. Acta* **2023**, *719*, 179384. [Crossref]
27. Vyazovkin, S.; Burnham, A. K.; Favergeon, L.; Koga, N.; Moukhina, E.; Pérez-Maqueda, L. A.; Sbirrazzuoli, N.; *Thermochim. Acta* **2020**, *689*, 178597. [Crossref]
28. Muravyev, N. V.; Pivkina, A. N.; Koga, N.; *Molecules* **2019**, *24*, 2298. [Crossref]
29. ASTM International; *E698-05: Standard Test Method for Arrhenius Kinetic Constants for Thermally Unstable Materials*; ASTM International: West Conshohocken, 2005. [Link] accessed in April 2024
30. Kissinger, H. E.; *Anal. Chem.* **1957**, *29*, 1702. [Crossref]
31. Vyazovkin, S.; *J. Comput. Chem.* **2001**, *22*, 178. [Crossref]
32. Friedman, H. L.; *J. Polym. Sci., Part C: Polym. Symp.* **1964**, *6*, 183. [Crossref]
33. Pérez-Maqueda, L. A.; Criado, J. M.; Sánchez-Jiménez, P. E.; *J. Phys. Chem. A* **2006**, *110*, 12456. [Crossref]
34. Vyazovkin, S.; Burnham, A. K.; Criado, J. M.; Pérez-Maqueda, L. A.; Popescu, C.; Sbirrazzuoli, N.; *Thermochim. Acta* **2011**, *520*, 1. [Crossref]
35. Vyazovkin, S.; Burnham, A. K.; Favergeon, L.; Koga, N.; Moukhina, E.; Pérez-Maqueda, L. A.; Sbirrazzuoli, N.; *Thermochim. Acta* **2020**, *689*, 178597. [Crossref]